Jurnal Polimesin
Department of Mechanical Engineering
State Polytechnic of Lhokseumawe
http://e-jurnal.pnl.ac.id/polimesin
e-ISSN : 2549-1999 No. : 6 Month : December
p-ISSN : 1693-5462 Volume : 22 Year : 2024

Article Processing Dates: Received on 2024-10-07, Reviewed on 2024-11-20, Revised on 2024-11-19, Accepted on 2024-11-20 and Available online on 2024-12-30

Structural failure study of truck rear wheel drive axle with defect variation using finite element method

Ulil Rizki[1], Husaini[2,*] dan Nurdin Ali[2]
[1]Department of Mechanical Engineering, Universitas Syiah Kuala, Banda Aceh, 23111, Indonesia
[2]Computational Mechanics Laboratory, Department of Mechanical Engineering, Universitas Syiah Kuala, Banda Aceh, 23111, Indonesia
*Corresponding author: husainiftm@usk.ac.id

Abstract

A truck is a major form of transporting goods on land because of its efficiency in terms of cost and effectiveness. Increased truck usage has heightened the risk of component failure, particularly in the rear-wheel-drive axle, which is prone to structural problems. Therefore, this study aimed to analyze the causes of rear-wheel-drive axle failure in trucks through numerical simulations based on the finite element method, using Finite Element Modeling and Postprocessing (FEMAP) software. The axle material used was AISI 4140, with four test models, including a version without defects and three other models with variations in defects at certain locations. During the investigation, the analysis was conducted to observe the effect of stress on axle performance under various defect conditions. The simulation results showed the maximum von Misses stress on the shaft without defects reached 115.19 MPa, which was significantly lower than the yield strength limit of 415 MPa of the material. The maximum shear stress of 124.67 MPa also remained lesser compared to the material allowable limit of 239.45 MPa, showing that the shaft was safe in a condition without defects. However, in the shaft model with defects, stress intensity factor (K_I) values were recorded at 17.80, 15.01, and 20.325 MPa.m$^{1/2}$, which exceeded the material fracture toughness (K_{IC}) value of 10 MPa.m$^{1/2}$. The results signified that $K_I > K_{IC}$ condition, facilitating accelerated crack propagation on the shaft, showing the potential for structural failure. This study provided a deep understanding of the importance of defect mitigation to maintain the reliability and safety of truck operations.

Keywords:
Structural failure, drive shaft, finite element method, stress intensity factor, fracture toughness.

1 Introduction

The use of trucks as a means of transportation is growing rapidly these days [1]. As a flexible land vehicle [2], a truck can transport various types of loads and play an important role in supporting economic activities in terms of goods distribution. The growing dependence on trucks [3] has led to an increase in various problems related to the failure of important components in the vehicle. Following the discussion, a critical component often raising concern is the rear-wheel-drive axle [4], which serves as the foundation for the drive system of the truck. This component is responsible for transmitting power from the engine to the rear wheel, allowing the vehicle to move and operate efficiently [5].

Rear wheel drive axle is a major element in truck system that plays an important role in maintaining the mobility and holding capacity of the vehicle [6]. Fig. 1 shows that axle is a component that serves by connecting power from the engine to rear wheel of the vehicle [7]. This component also functions by moving truck and distributing the load optimally [8].

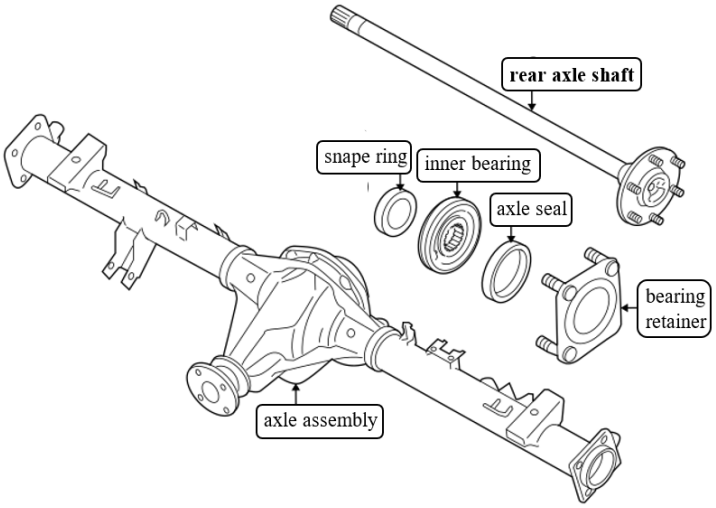

Fig. 1. Axle is a part that drives rear wheel of truck [9].

As the component failures of rear-wheel-drive axles in trucks become increasingly common and widespread, a detailed analysis incorporating different methods and perspectives is required to identify the various failure points [10].

The finite element method was used to conduct loading simulations in some investigations. In the study of Fauzan *et al.* [5], failure analysis was performed only on the defect area located near axle teeth (splines) on the wheel drive axle, while the investigation by Qarnul *et al.* [11], analyzed the broken area of the axle near the axle lip (flange).

This study conducted a simulation-based failure analysis on the rear axle of a truck with various loading scenarios at various locations. The loading scenarios included rear axle conditions in normal conditions without defects and conditions with initial defects at three different locations. This follow-up investigation aimed to understand the influence of defect conditions on stress distribution, deformation, and crack potential in truck rear wheel drive axles.

2 Study Materials and Methods

2.1 Material

The material used in this study was a rear wheel drive axle on a truck with a total length of 805 mm and a diameter of 35 mm. A 150 mm diameter flange was located at one end of the axle, acting as an interface for connecting the material and other components. This axle was also equipped with 18 splines as a power distributor. According to previous studies, the rear axle of the truck was made from a material classified as AISI 4140 [11]. This material was known as an alloy steel with excellent mechanical properties, specifically in applications that required high strength, toughness, and fatigue resistance [12]. The chemical composition of AISI 4140 material was shown in Table 1.

Table 1. Chemical composition of AISI 4140 material [11]

Element	Composition (%)
Carbon (C)	0.38 - 0.43
Chromium (Cr)	0.80 - 1.10
Manganese (Mn)	0.75 - 1.00
Molybdenum (Mo)	0.15 - 0.25
Silicon (Si)	0.15 - 0.30
Phosphorus (P)	max. 0.035
Sulfur (S)	max. 0.040

The main elements, such as chromium and molybdenum contributed significantly to corrosion resistance and wear resistance, while carbon increased the strength and hardness of the material. Manganese played a role in increasing tensile strength, and silicon increased the elasticity of steel [13]. Following this discussion, the mechanical properties of AISI 4140 material were shown in Table 2.

Table 2. Mechanical properties of AISI 4140 material [14]

Properties	Value
Ultimate strength, σ_B	655 MPa
Yield strength, σ_y	415 MPa
Elastic modulus, E	190-210 GPa
Shear modulus, G	80 GPa
Poisson's ratio, v	0.27-0.30
Fracture toughness, K_{IC} [15]	10 MPa.m$^{1/2}$

The rear-wheel-drive axle of the truck fabricated from AISI 4140 material, offered high torque transmission capabilities with excellent resistance to fatigue and wear. By applying an optimal heat treatment process, the axle is strengthened to withstand various extreme operational conditions such as heavy loads, vibrations, and high speeds [16].

2.2 Study Methods

Previous studies conducted investigations using experimental methods to determine the material type of the rear wheel drive axle [11]. The methods included hardness testing, chemical composition testing, microstructure observation, and visual surface observation.

During this study, stress analysis was performed with the finite element method using Finite Element Modeling and Postprocessing (FEMAP) software version 12.0.1. A tetrahedral mesh with a size of 0.1 mm was used in the numerical simulation, producing a total of 57,316 and 361,397 nodes. This configuration was selected to obtain precise and accurate analysis results in describing stress distribution as well as deformation on the rear-wheel-drive axle of the truck.

The simulation process in this investigation aimed to identify stress distribution and stress intensity factor (K_I) on the rear axle of the vehicle. During this study, four different axle models, namely an axle model without defects as the initial condition and three models with initial defects at three different locations, were used.

The four models of rear wheel drive axles for truck included:

1. Model of drive axle without defects.
2. A model with an initial defect of 665 mm from axle teeth (point A, shown in Fig. 2).
3. Model of drive axle with an initial defect of 335 mm from axle teeth (point B, shown in Fig. 2).
4. A model with an initial defect of 95 mm from axle teeth (point C, shown in Fig. 2).

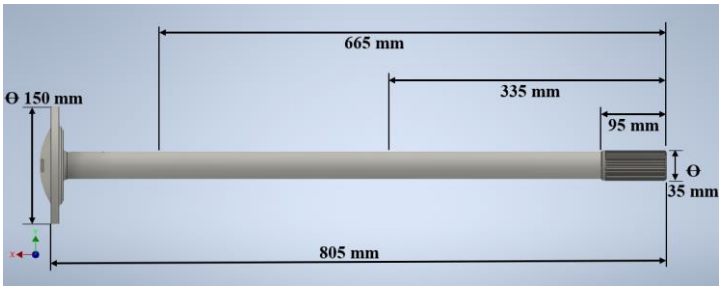

Fig. 2. Rear wheel drive axle of truck.

The simulation began by entering the redesigned shaft geometry using Computer-Aided Design (CAD) software into FEMAP software in the first model. Subsequently, simulation and loading analysis were conducted to determine the von Mises stress value as well as maximum shear stress, which were then compared to the yield strength value (σ_y) and the material allowable shear stress (τ_{izin}) of the material [17]. Yield strength value (σ_y) of the material was obtained from the previous test shown in Table 2, while the allowable shear stress value (τ_{izin}) of the material was determined from the calculation of Eq. 1 [18].

$$\tau_{izin} = 0.577 \times \sigma_y = 239.45 \text{ MPa} \quad (1)$$

where σ_y represented the yield strength of the material (MPa).

A simulation process was conducted in the drive axle model with initial defects at points A, B, and C. These defects were used to analyze stress values that occurred in axle elements, where the variable data were determined by calculating K_I value. In addition, K_I value can be calculated using Eq. 2 [19].

$$K_I = \frac{\sigma_{xx}\sqrt{2\pi r}}{\cos\left(\frac{\theta}{2}\right)\left[1-\sin\left(\frac{\theta}{2}\right)\times\sin\left(\frac{3\theta}{2}\right)\right]} \quad (2)$$

where:
K_I = Stress intensity factor (MPa.m$^{1/2}$)
σ_{xx}= Stress (MPa)
r = Distance from crack tip to node point (m)
θ = The angle formed

K_I was compared with the material fracture toughness (K_{IC}) value to determine the enlargement or reduction of the crack. This analysis was performed to assess the performance of the material under load, specifically in scenarios where defects or cracks occurred. The relationship between K_I and K_{IC} values was critical, where exceeding K_{IC} value led to crack as well as failure [20-21], while a lower K_I variable ensured the crack remained safe and stable.

3 Results and Discussion

3.1 Analysis of the Flawless Drive Axle Model

The condition of the shaft without defects in the first model signified a normal load distribution with a maximum von Mises stress value of 115.19 Mpa. Fig. 3 showed that the fillet area experienced the highest von Mises stress value distribution.

The calculated von Mises stress value was significantly lower when compared to the yield strength of the material, which was 415 MPa. This comparison showed that the maximum von Mises stress in the first model remained in acceptable limits.

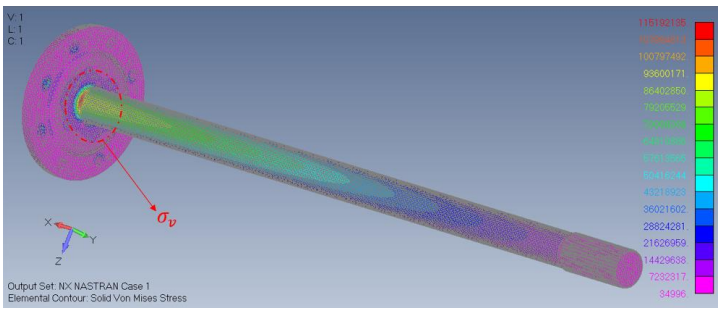

Fig. 3. von Mises stress.

The maximum shear stress results in the simulation signified a centralized location in the fillet area with a value of 124.67 MPa as shown in Fig. 4. The analysis results confirmed that the calculated value did not exceed the allowable shear stress limit of the material, which was 239.45 MPa, as determined through the calculations in Eq. 1.

The results showed that the rear-wheel-drive axle structure was safe since the shear stress value was lesser than shear stress limit

permitted by the material. This outcome signified that the material possessed a sufficient safety margin to withstand shear stress that occurred.

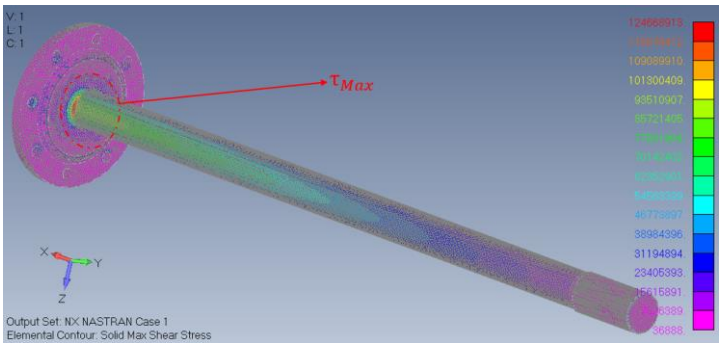

Fig. 4. Maximum shear stress.

3.2 Drive Axle Model with Initial Defects had a Length of 665 mm from Axle Teeth (Point A)

The initial defect condition at point A in the second model was shown in Fig. 5. The analysis results signified an increased load distribution in the area around the defect with a maximum von Mises stress value of 42.41 MPa.

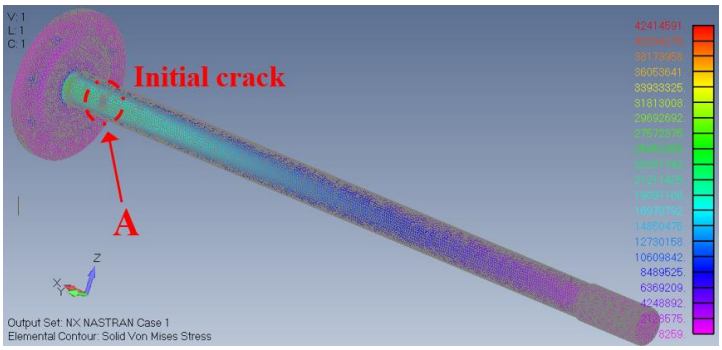

(a)

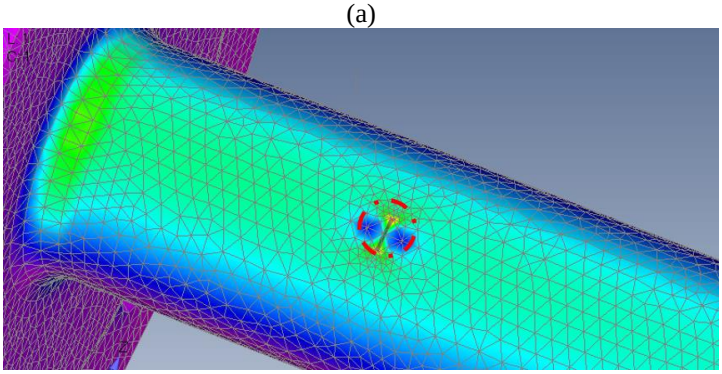

(b)

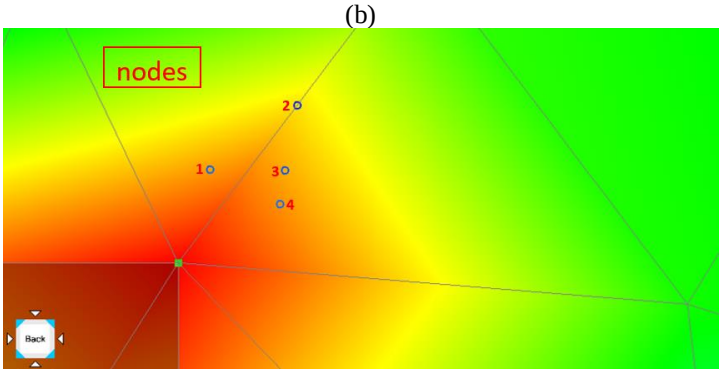

(c)

Fig. 5. (a) Simulation of drive axle with FEMAP model A, (b) enlargement of the defect location, (c) nodes locations around the defect.

K_I analysis in Table 3 showed an average value of 17.80 MPa.m$^{1/2}$. This value was higher when compared to the K_{IC} value of 10 MPa.m$^{1/2}$. Moreover, the results signified that the rear wheel drive axle of the truck experienced crack propagation and failure.

Table 3. Results of K_I calculations for the second defect model at point A.

Nodes	σ_{xx} (MPa)	r	θ	K_I (MPa.m$^{1/2}$)
399413	38.17	0.007	71	22.18
370889	36.05	0.015	52	21.55
340923	38.17	0.011	41	15.47
472804	40.29	0.009	29	11.95
Average				17.80

3.3 Drive Axle Model with Initial Defects had a Length of 335 mm from Axle Teeth (Point B)

As shown in Fig. 6, the third model, with an initial defect at point B, signified a load concentration around the defect area, leading to a von Mises stress value of 50.09 MPa.

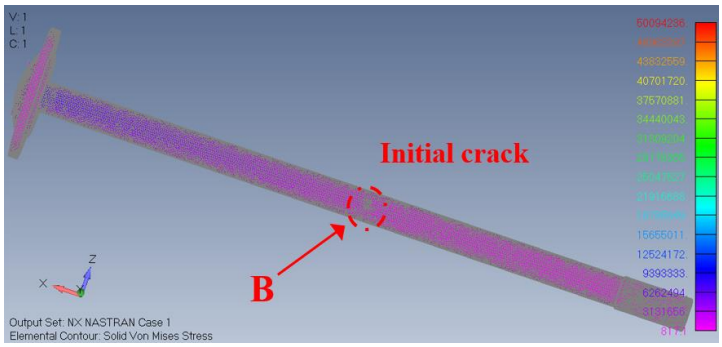

(a)

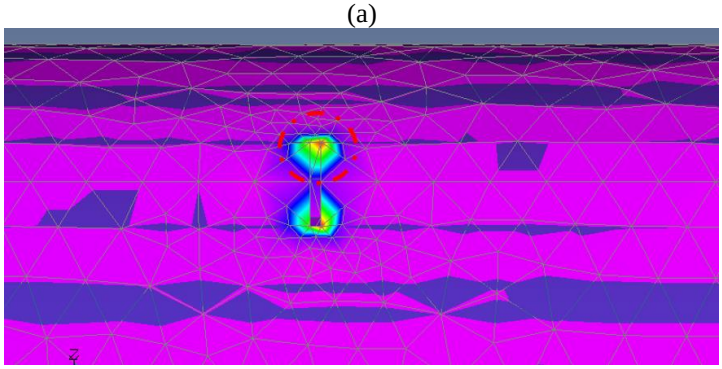

(b)

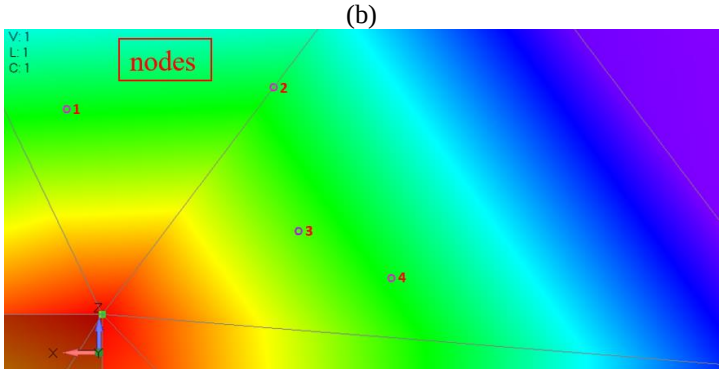

(c)

Fig. 6. (a) Simulation of drive axle with FEMAP model B, (b) enlargement of the defect location, (c) nodes location in the defect area.

Fig. 6 showed that the defect area experienced the highest von Mises stress value distribution. During the study, K_I calculated in Table 4 had an average value of 15.01 MPa.m$^{1/2}$, which exceeded the K_{IC} value of 10 MPa.m$^{1/2}$. This result signified that the shaft experienced increased crack propagation.

Table 4. Results of calculating K_I for the three defect models in the area of point B.

Nodes	σ_{xx} (MPa)	r	θ	K_I (MPa.m$^{1/2}$)
296108	31.30	0.011	100	20.74
270557	28.17	0.015	53	17.21
288946	37.57	0.011	23	11.36
385093	34.44	0.015	7	10.71
Average				15.01

3.4 Drive Axle Model with Initial Defects is Given 95 mm from Axle Teeth (Point C)

The initial defect in the fourth model was applied at the location of point C as shown in Fig. 7. Based on the simulation results, the maximum load distribution was centered around the defect. This condition signified that defects affected the stress distribution pattern in the surrounding area. The maximum von Mises stress value of 49.30 MPa obtained from the simulation implied that areas with defects were more prone to failure. Moreover, the results of K_I analysis in Table 5 showed an average value of 20.33 MPa.m$^{1/2}$. Exceeding K_{IC} value, this result signified that the shaft experienced significant crack propagation, eventually leading to failure.

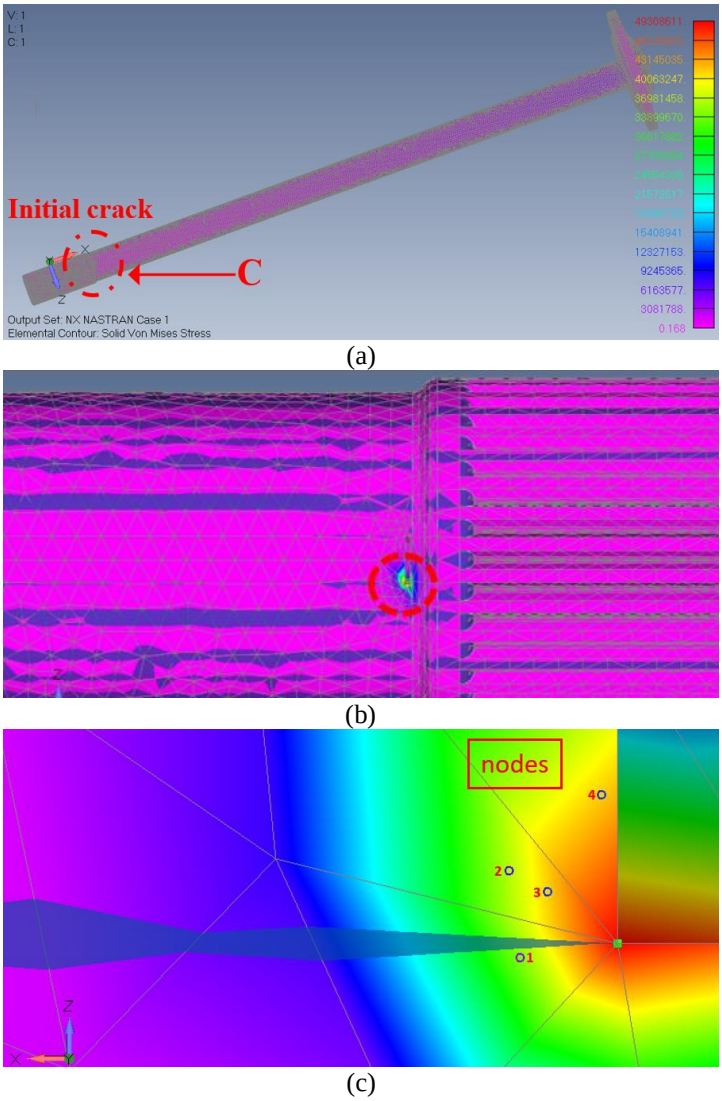

(a)

(b)

(c)

Fig. 7. (a) Simulation of drive axle with FEMAP model of defect model C, (b) enlargement of the defect location, (c) location of nodes assignment in the defect area.

Table 5. Results of calculating K_I for the fourth model

Nodes	σ_{xx} (MPa)	r	θ	K_I (MPa.m$^{1/2}$)
166330	33.89	0.010	98	21.98
187176	40.63	0.013	56	24.66
196675	43.14	0.009	54	20.87
179450	43.14	0.016	5	13.76
Average				20.33

The results of the analysis showed that the three models with initial defects experienced further crack propagation as the applied stress exceeded the K_{IC} value of the axle material. This crack was caused by high stress exceeding the safe limit that was accepted by the drive axle. Fig. 8 showed the comparative relationship between K_1 and K_{IC} values of three rear-wheel-drive axle models with initial deformed conditions.

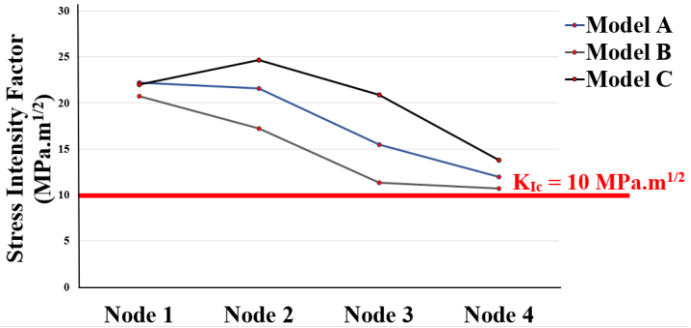

Fig. 8. Graph of the relationship between K_I and K_{IC} of A, B as well as C axis models.

A previous study conducted by Fauzan *et al.* [5] investigated the rear-wheel-drive axle of a truck using an experimental method, producing valuable results. The study found that the cause of failure was due to initial defects in the splines area. In addition, shear stress analysis showed that the maximum shear stress exceeded the permissible shear stress on axle material.

During this study, a stress analysis was conducted using the finite element method on the shaft by modeling several initial defects at different locations to find K_I. Subsequently, the value was compared with K_{IC} of the shaft material as shown in Fig. 8.

4 Conclusion

The simulation-based analysis failure analysis on the rear axle of a truck with four models showed the relationship between the location of the defects on the shaft and the severity of the potential failure.

1. The first model, representing a defect-free shaft, provided a benchmark with von Mises stress and shear stress values of 115.19 MPa and 124.67 MPa, respectively. These values were significantly below the material limit with a yield stress of 415 MPa and allowable shear stress of 239.45 MPa.
2. Analysis of the defect impact on the shaft with initial defects, particularly around the splines, revealed that the stress intensity factor (KI) exceeded the fracture toughness (KIC) of AISI 4140 material by 10 MPa·m$^{1/2}$, highlighting a critical risk for crack propagation.
3. Analysis of the stress intensity factor revealed the average KI values for the three defect models were 17.80 MPa·m$^{1/2}$, 15.01 MPa·m$^{1/2}$, and 20.33 MPa·m$^{1/2}$. These results underscored the strong correlation between defect location and the potential severity of failure.

Acknowledgments

The authors are grateful to the Universitas Syiah Kuala for their partial financial support through the Research Grant No. 89/UN11.2.1/PG.01.03/SPK/PTNBH/2024. The authors are also grateful to the Computational Mechanics Laboratory and Department of Mechanical Engineering, Universitas Syiah Kuala, Banda Aceh, for making the facilities accessible.

References

[1] J. Gnap, T. Settey, dan L. Baloghová, "Examination of the development of the number and use of trucks up to 3.5 tons total weight," *Transportation Research Procedia*, vol. 55, hlm. 1-10, 2021.

[2] F. Chen, M. Song, X. Ma, dan X. Zhu, "Assess the impacts of different autonomous trucks' lateral control modes on asphalt pavement performance," *Transportation Research Part C: Emerging Technologies*, vol. 98, hlm. 10-25, 2019.

[3] M. Wozniak, G. Ozuna, dan K. Siczek, "The Study on the Damage of the Rear-Axle Shaft in a KIA Truck," *Advances in Science and Technology Research Journal*, vol. 14, no. 2, hlm. 115-124, 2020.

[4] B. Zheng, S. Fu, dan J. Lei, "Topology optimization and multiobjective optimization for drive axle housing of a rear

axle drive truck," *Materials*, vol. 15, no. 15, hlm. 5268, 2022.
[5] H. Husaini, Fauzan, N. Ali, dan A. Arhami, "Failure Analysis of the Rear Driveshaft Using Experimental and Analytical Methods," *AIP Conference Proceedings*, vol. 2613, 2023.
[6] H. Isworo dan W. A. Pratama, "Failure Analysis of Rear Wheel Axis (Case Study) on Truck X," *Jurnal Tugas Akhir Mahasiswa – Rotary*, vol. 4, hlm. 102-114, 2022.
[7] P. K. Teja, G. Moorthy, dan S. Kaliappan, "Finite Element Analysis of Propeller Shaft for Automotive and Naval Application," *International Research Journal of Automotive Technology*, vol. 1, hlm. 8-12, 2018.
[8] L. H. Zhao, Q. K. Xing, J. Y. Wang, S. L. Li, dan S. L. Zheng, "Failure and root cause analysis of vehicle drive shaft," *Engineering Failure Analysis*, vol. 102, hlm. 38-49, 2019.
[9] Gasket and Sealing System. Diakses dari https://parts.dickhannahnissan.com/v-2013-nissan-titan--s--5-6l-v8-flex/driveline-and-axles--gaskets-and-sealing-systems (diakses pada 08 November 2024).
[10] M. Syahril, "Analisis Kegagalan Poros Roda Belakang Kendaraan," *Majalah Metalurgi*, vol. 139, hlm. 139-148, 2013.
[11] M. Qarnul, "Analisis Kegagalan Poros Penggerak Roda Belakang Truk 125 PS Menggunakan Metode Eksperimental dan Numerikal," Skripsi, Jurusan Teknik Mesin dan Industri, Fakultas Teknik, Universitas Syiah Kuala, 2023.
[12] M. Badaruddin, S. Sumardi, dan D. Asmi, "Improvement of the fatigue crack growth resistance in AISI 4140 steel under single-and multi-austempering heat treatments," *Results in Engineering*, Elsevier, 2024.
[13] M. M. Bilal, K. Yaqoob, M. H. Zahid, W. H. Tanveer, *et al.*, "Effect of austempering conditions on the microstructure and mechanical properties of AISI 4340 and AISI 4140 steels," *Journal of Materials*, vol. 9, no. 4, hlm. 345-356, 2019.
[14] V. Naranje dan S. Salunkhe, "Experimental investigation and numerical analysis of axle spline shaft analysis for different materials," *Materials Today: Proceedings*, vol. 59, hlm. A14-A21, 2022.
[15] K. M. P. Rao dan K. N. Prabhu, "Numerical simulation to predict the effect of process parameters on hardness during martempering of AISI4140 steel," *Journal of Materials Engineering and Performance*, vol. 30, no. 4, hlm. 1965-1976, Springer, 2021.
[16] M. A. Erden dan B. Ayvacı, "The effect on mechanical properties of pressing technique in PM steels," *Acta Physica Polonica A*, vol. 136, hlm. 256-261, 2019.
[17] Husaini, Osama, dan T. E. Putra, "The analysis of crankshaft failure in a 2,500 cc diesel engine vehicle using experimental method," *International Conference on Experimental and Computational Mechanics in Engineering*, hlm. 123-130, Springer, 2021.
[18] W. Saiful, H. Husaini, dan N. Ali, "Failure analysis on the fracture shaft of a centrifugal pump used for diesel engine cooling system," *Key Engineering Materials*, vol. 892, hlm. 107-114, 2021.
[19] H. Husaini, *Dasar-Dasar Mekanika Retakan*, Banda Aceh: Syiah Kuala University Press, 2015.
[20] H. Husaini, R. Anshari, N. Ali, dan J. Yunus, "The analysis of the failure of leaf spring used as the rear suspension system in 110 PS diesel trucks," *AIP Conference Proceedings*, vol. 2613, 2023.
[21] H. Husaini, T. E. Putra, dan S. Novriandika, "Study of Failure Analysis of a Fracture Crankshaft Pulley Used on a Truck Engine," *IOP Conf. Series: Materials Science and Engineering*, vol. 739, hlm. 012-018, 2020.
[22] H. Husaini, T. E. Putra, dan Zulfikar, "Analysis of Cracks on a Fractured Surface of the Vehicle Crankshaft Using the Finite Element Method," *International Journal of Engineering & Technology*, vol. 7, hlm. 1564-1568, 2019.